Development of a Universal NADH Detection Assay for High Throughput Enzyme Evolution Using Fluorescence Activated Droplet Sorting

Working Paper

Author(s):
Kolaitis, Gerassimos; Jain, Ankit; Romeis, Dennis; Buryska, Tomas; Steiger, Matthias; Wuerstl, Lena; Doering, Manuel; Beer, Barbara; Stavrakis, Stavros; deMello, Andrew; Sieber, Volker

Publication date:
2022-07-07

Permanent link:
https://doi.org/10.3929/ethz-b-000612982

Originally published in:
ChemRxiv, https://doi.org/10.26434/chemrxiv-2022-jvg5j

Funding acknowledgement:
176011 - Advanced Droplet-Based Technologies for Engineering Dynamic Elements in Proteins (SNF)

Development of a Universal NADH Detection Assay for High Throughput Enzyme Evolution Using Fluorescence Activated Droplet Sorting

Gerassimos Kolaitis [a,c], Ankit Jain [b], Dennis Romeis [a], Tomas Buryska [b], Matthias Steiger [a,c], Lena Wuerstl [a], Manuel Doering [a], Barbara Beer [a,d], Stavros Stavrakis [b], Andrew DeMello [b] and Volker Sieber *[a,c,e,f]

a. Chair of Chemistry of Biogenic Resources, Technical University of Munich, Campus Straubing for Biotechnology and Sustainability, Schulgasse 16, 94315 Straubing, Germany

b. Institute for Chemical and Bioengineering, Department of Chemistry and Applied Biosciences, ETH Zürich, Vladimir Prelog Weg 1, 8093 Zürich, Switzerland

c. Catalysis Research Center, Technical University of Munich, Ernst-Otto-Fischer-Strasse 1, 85748 Garching, Germany

d. Current address: CASCAT GmbH, Europaring 4, 94315 Straubing

e. Straubing Branch BioCat, Fraunhofer IGB, Schulgasse 11a, 94315 Straubing, Germany

f. School of Chemistry and Molecular Biosciences, The University of Queensland, 68 Copper Road, St. Lucia 4072, Australia

ABSTRACT: Directed evolution is an enzyme engineering approach based on the generation and screening of large mutagenesis libraries, with a view to discovering enzymes with improved properties such as activity, specificity or stability. Recently, droplet-based microfluidics has emerged as a powerful technology enabling ultra-high throughput screening of enzyme libraries and the effective identification and isolation of novel, improved enzyme variants, outperforming conventional enzyme screening platforms by several orders of magnitude in terms of speed and chemical consumption. When using droplet-based platforms fluorescence remains the predominant choice for detection of enzymatic activity due to its high sensitivity and low limits of detection. However, this approach often requires the use of labeled, non-natural substrates, which are typically not commercially available. In addition, fluorescence detection is only suitable for a few enzyme classes such as hydrolases or oxidases, whose reactions can often lead to a fluorescent signal. Herein, we describe an assay that enables fluorescence detection of enzymatic activity through a reaction cascade for the industrially important enzyme subclass of dehydrogenases. By applying a hydrogen peroxide-forming NADH oxidase coupled with peroxidase-catalyzed fluorescence generation, quantification of NADH and dehydrogenase activity becomes possible. We explored the utility of this assay in the evolution of a low performing alcohol dehydrogenase from *Sphingomonas species A1* (*Sps*ADH). A fluorescence-activated droplet sorting (FADS) platform was utilized for the screening of a 50,000 variant *Sps*ADH library towards the non-native substrate L-guluronate, a primary component of macroalgae, with the potential to serve as raw material for the bio-based production of chemicals. Significantly, we found an enzyme variant with a 2.6-fold improvement in catalytic efficiency kcat/Km towards the non-native substrate, with only a single round of mutagenesis. The screening of *Sps*ADH libraries confirms the ability of the developed method to enrich active enzyme variants.

KEYWORDS: Enzyme Engineering, FADS, Microfluidics, NADH Oxidase, Guluronate, Seaweed, Assay

Biocatalysis is an important aspect in the development of new sustainable chemical processes. It utilizes single enzymes, enzyme cascades and entire metabolic networks within cells.[1–3] A key challenge in the development of a biocatalytic process is the identification of suitable enzymes. As naturally occurring enzymes are often suboptimal for technical use, enzyme engineering is invaluable in enhancing their properties and tailoring them to the requirements of a specific biotechnological application.[4–7] Enzyme engineering approaches, such as *in silico* supported rational design have succeeded in improving protein stability and binding affinity of substrates. To this end, Google´s *Alpha Fold* holds much promise for substantially accelerating enzyme engineering through its ability to generate structural data at high speed.[8–12] In addition, other computational predictive algorithms based on machine learning have shown to efficiently generate genetic diversity in directed evolution campaigns.[13,14] However, adoption of these approaches cannot lead to candidates with high turnover numbers k_{cat}, since this requires complex simulations, not only of the transition state of the catalyzed reaction, but also of the dynamics of the active site and the entire enzyme. To overcome this limitation, directed evolution (DE) is still the method of choice to create enzymes with desired properties. In directed evolution, thousands to millions of variants of a single protein are created, with those showing improved traits being selected for further study.[15] The larger the number of variants generated, the larger the proportion of the sequence space that is sampled and the higher the probability of obtaining an enzyme variant with sufficiently improved properties.

Unfortunately, traditional screening platforms that monitor mutant activity on agar or in microwell plates are laborious and low throughput (between 10^4 and 10^5 screens per day at best).[16] In the past few years, droplet-based microfluidic technologies have emerged as a powerful tool for high-throughput enzyme engineering and other applications.[17,18] Such approaches are exceptionally well suited for performing large numbers of discrete experiments on

small sample volumes. The adoption of a segmented flow regime allows the compartmentalization of an analyte within pL-volume droplets that reside within a continuous and immiscible carrier fluid. In addition, such platforms enable the processing of monodisperse droplets at kilohertz rates and provide for precise control over each droplet in terms of its size and chemical payload. Specifically, substrate and bacteria containing protein(s) of interest and their coding gene(s) are co-compartmentalized within a droplet, allowing genotype and phenotype to become linked in a simple manner. Custom-built droplet-based microfluidic sorting devices based on fluorescence signals have been applied successfully for screening large enzyme variant libraries.[19–21] One of the early attempts to implement this technology in screening large populations of enzyme was in the directed evolution of horseradish peroxidase (HRP). The HRP gene encoded on a plasmid as a fusion to Aga2 gene allowed its surface display on yeast cells. For screening peroxidase activity, the conversion of the substrate (Amplex UltraRed) using H_2O_2, to a fluorescent product (resorufin) was observed.[22] Specifically, pL-volume droplets containing single yeast cells were formed and dielectrophoretically sorted at kilohertz frequencies to yield a population of droplets containing the most active enzymes. The sorting strategy referred to as "Fluorescence Activated Droplet Sorting" (FADS) involves assessing enzymatic efficiency through measurement of the time-integrated fluorescence signal originating from individual droplets.

To date, FADS has been utilized for the directed evolution of enzymes of the enzyme commission (EC) class of hydrolases[21,23–25] and the EC subclass of oxidases.[20,22,26] The latter form hydrogen peroxide that generates a fluorescence signal via oxidation of a precursor (as described in the example above).[22] For the former, several fluorogenic surrogate substrates have been synthesized[27–30] and applied in metagenomic mining of promiscuous hydrolases, or been used for the validation of DE methods in FADS platforms.[21,31,32] However, since surrogate substrates usually differ from those of the actual target reaction in DE, the aforementioned FADS approaches are limited to a "proof of concept" studies, going as far as "making important what's measurable" instead of "making measurable what's important."

As an alternative to FADS, an absorbance-activated droplet sorting (AADS) platform was recently reported and applied to a subclass of dehydrogenases.[34] Enzymes of this subclass have found wide application in the synthesis of chiral alcohols or amines and in the utilization of biogenic resources.[35,36] About 90 % of industrially applied dehydrogenases use NADH or NADPH as a cofactor, whose absorbance can be monitored at 340 nm.[37] Accordingly, NAD(P)H has long been utilized as a detection probe for a multitude of enzymatic reactions as well as analytes. By simply coupling several highly specific enzyme reactions to the formation or conversion of NAD(P)H, the concentration of an analyte or the activity of the enzyme of interest can be monitored. The universality of this approach led to the development of the "Boehringer Mannheim Methods of Analysis", that became the key component of numerous commercial kits for analyzing several organic and inorganic compounds (**Figure 1A**).[38,39] Accordingly, the detection of NAD(P)H formation or its conversion has been widely used in enzyme engineering, not only for oxidoreductases but also, in coupled assays for other enzymes classes.[40–43] Whilst the extinction coefficient of NADH (6220 M^{-1} cm^{-1}) provides a good basis for absorbance detection in cuvette and microplate spectrophotometers, its detection in microfluidic systems is hindered by the short optical pathlengths associated with pL-volume droplets.[44] By oxidizing NADH with water-soluble tetrazolium salts (WST-1) using an electron mediator, brightly colored formazans are formed with high extinction coefficients in the visible light spectrum (**Figure 1B**, left).[45] To overcome limitations in absorbance sensitivity, Gielen *et al.* implemented such an approach in their AADS platform, allowing the screening of improved phenylalanine dehydrogenase variants at a rate of 300 droplets per second.[34] Given that the concentration limit of detection of WST-1 in AADS is 10 µM[34] and assuming an incubation time of one hour, AADS is best suited for dehydrogenases with specific activities of about 10 U mg^{-1} and above (for details, see **Section S2**).[46] Therefore, for screening low-performing enzymes highly sensitive fluorescence-based assays are required.[47–49]

Recently we identified a promiscuous enzyme that is capable of oxidizing L-guluronic acids to glucaric acid (**Scheme 1**) in *Sphingomonas species* A1 (*Sps*ADH). Its native reaction is the reduction of 4-deoxy-L-erythro-5-hexoseulose uronic acid to 2-keto-3-deoxy-D-gluconate.[50] L-guluronic acid is a major constituent of seaweeds,[51] while glucaric acid is among the U.S. Department of Energy's top 12 biobased chemicals and an interconversion would be desirable.[52] Several uronate dehydrogenases have been previously reported for their potential to oxidize several D-uronic acids such as D-mannuronic, D-glucuronic, and D-galacturonic acid.[53] However, to our knowledge, no enzyme has been reported that sufficiently accepts L-guluronic acid as a substrate for oxidation to glucaric acid. With a specific activity of about 15 mU mg^{-1} against L-guluronic acid (**Figure S1**), utilization AADS for optimizing *Sps*ADH activity is not suitable. On the other hand, neither the product nor the produced NADH of the catalyzed reaction exhibit high fluorescence. Accordingly, we sought to combine NAD(P)H formation with a fluorescence signal that is bright enough to increase the sensitivity of FADS measurements.

Scheme 1: Aldehyde dehydrogenase side activity of *Sps*ADH in the oxidation of L-guluronic acid to d-glucaric acid

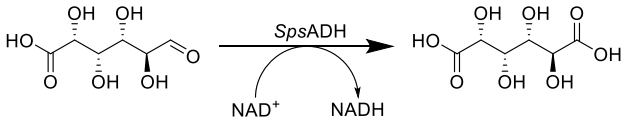

Herein, we first describe a fluorescence-based assay for measuring the activity of NADH-producing enzymes in pL-volume droplets. It is based on the oxidation of Amplex UltraRed by HRP using H_2O_2 produced by an NADH-oxidase (**Figure 1B**). It can be applied for enzymes with specific activities as low as 0.06 mU mL^{-1}. We tested the applicability of this assay for DE experiments utilizing FADS. More specifically, a random mutagenesis library of the whole

gene with 50,000 enzyme variants of *Sps*ADH was expressed in *Escherichia coli* and single bacterial cells were encapsulated in microfluidic droplets. After one round of screening, an enzyme variant with a 2.6-fold improvement in catalytic efficiency k_{cat}/K_m towards the non-native substrate, L-guluronic acid, was identified compared to the template enzyme. Since the detection and quantification of NAD(P)H is the basis for many reactions and analytes (**Figure 1**), we believe that the current detection assay will significantly broaden the applicability of FADS in screening large mutagenic libraries beyond hydrolases and oxidoreductases.

RESULTS AND DISCUSSION

Characterization of a suitable NADH oxidase

For the generation of a fluorescent signal based on NADH formation from the enzyme of interest, a subsequent cascade reaction based on peroxidase-catalyzed oxidation of Amplex UltraRed to Resorufin with H_2O_2 was used (**Figure 1B** right panel). A key element of such an assay is an NADH oxidase (NOX) that produces hydrogen peroxide. Interestingly, even though many NADH oxidases have been characterized and used widely for the regeneration of the oxidized cofactor in biotechnological processes, most of them have an intrinsic catalase activity, which prohibits them from producing H_2O_2.[54] In addition, many commonly used NADH oxidases typically do not operate at their favorable pH when participating in coupled reactions, are thermally unstable and require an excess of externally supplied dithiothreitol and redox active coenzymes like FAD to operate.[55] These traits can render this class of enzymes unattractive for enzymatic assays toward enzyme engineering. Therefore, we first had to identify a suitable NADH oxidase with high stability and without catalase activity. To do so, we tested three previously published NADH oxidases from *Thermus thermophilus, Archaeoglobus fulgidus* or *Streptococcus mutans.*[56–58] The NADH oxidase from *T. thermophilus* HB8 (*Tt*NOx) is an H_2O_2 producing oxidase with low enzymatic activity at room temperature but with high thermostability up to 80°C[58] while the NADH oxidase from the hyperthermophilic sulfate-reducing anaerobe *A. fulgidus* (*Af*NOX), when expressed in *E. coli*, leads to a thermostable NADH oxidase with maximal catalytic activity at 80°C.[57] Higuchi et al. have identified two distinct NADH oxidases from *S. mutans*, with one of them being able to produce H_2O_2 with a maximal activity at 45°C (*Sm*NOX).[56]

Herein, we expressed all three genes for these NADH oxidases using a C- or N-terminal 6x poly-histidine tag in *E. coli* BL21(DE3) and analyzed the purified enzymes for their suitability in enzymatic assays. Their H_2O_2 production rate was measured and their activity was quantified at room temperature by coupling formation to the oxidation of ABTS (2,2'-azino-bis(3-ethylbenzothiazoline-6-sulfonic acid) catalyzed by horseradish peroxidase.[59] Surprisingly, *Tt*NOX and *Af*NOX did not show any H_2O_2 production (data not shown), probably due to their thermophilic

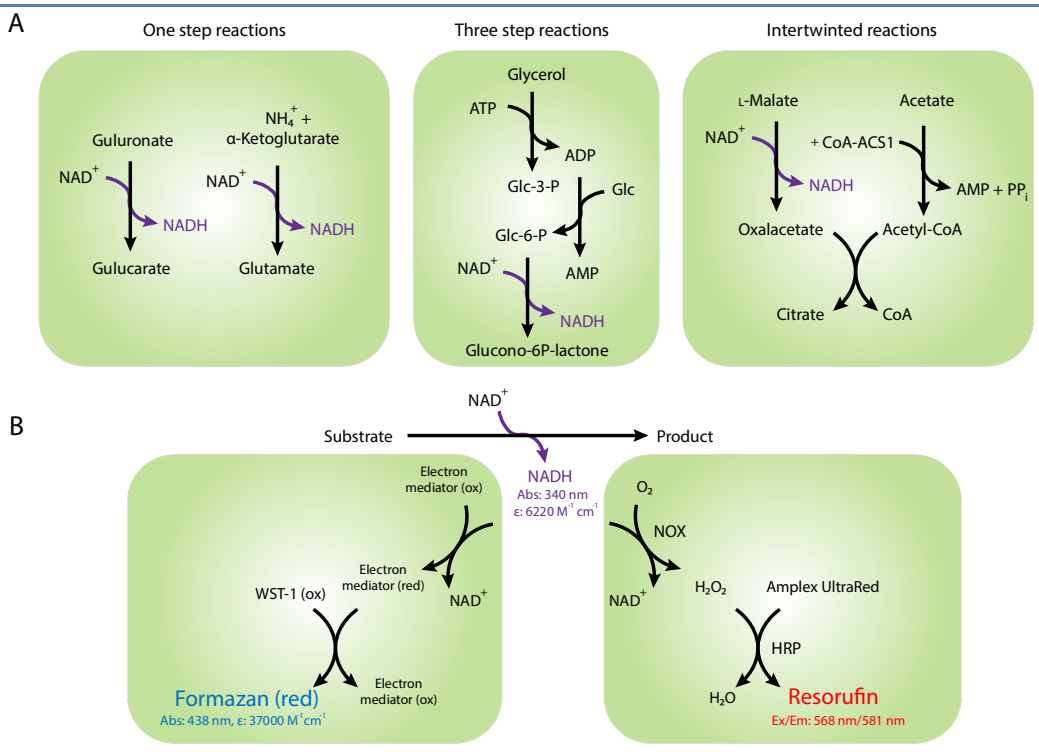

Figure 1. A) Examples of detection reactions via NADH production from the Boehringer Mannheim Methods of Analysis.[38,39] Glc stands for glucose, Glc-3-P for glucose-3-phosphate and Glc-6-P for glucose-6-phosphate. NADH production can be achieved by either one step reactions directly, intertwined reactions when the reaction from malate to oxalacetate is on the side of the malate and three step reactions. B) Systems for enhanced and more sensitive NADH detection. Left – WST-1 based absorption, right – resorufin based fluorescence. The enzyme of interest reduces NAD+ to NADH while performing its main reaction. Subsequently, NADH oxidase regenerates NADH to NAD+ and produces hydrogen peroxide. HRP uses hydrogen peroxide to reduce Amplex UltraRed and thereby produce a fluorescence signal.

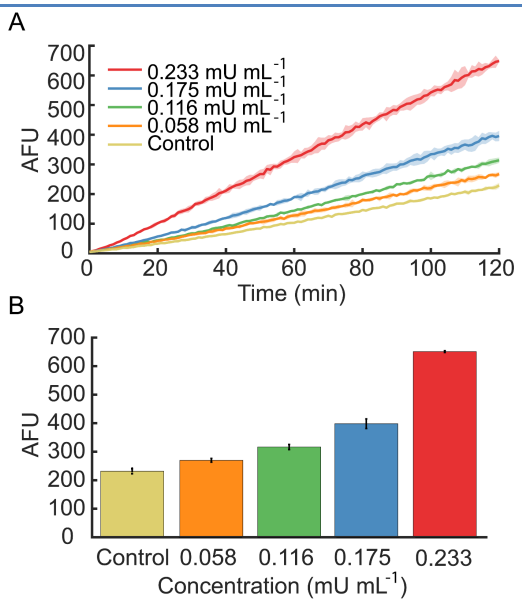

Figure 2. A microtiter plate optimization experiment assessing assay performance at varying SpsADH concentrations. The composition in the plate corresponds to a scaled up, occupied droplet. The transparent shading and error bars represent the standard deviation to the data measured in triplicate. A) Assay performance at varying levels of purified enzyme. The enzyme was not added to the control. B) The end-point fluorescence signal after 2 hours of incubation at lower enzymatic concentrations.

origin that leads to low activity at room temperature or to a previously unknown catalase activity. Therefore, these enzymes were not considered further. On the contrary, *Sm*NOX was able to produce H_2O_2 at different concentrations of NADH (**Figure S2A**). Interestingly, immediate formation of the oxidized form of the ABTS colorimetric dye could only be observed at low NADH concentrations due to the competing oxidation reaction of NADH by HRP (see **Section S3**). In light of this inhibition phenomenon, and to ensure the applicability of *Sm*NOX, we determined its kinetic data (K_m = 12.79 ± 2.78 µM, V_{max} = 0.35 ± 0.015 U mg^{-1}) (**Figure S3**). The relatively low K_m value is beneficial since the immediate conversion of NADH to NAD$^+$ after its formation is important for its regeneration as well as avoiding the potentially competing oxidation of NADH by HRP.

Construction and optimization of the assay for monitoring enzymatic activity in droplets.

As described previously, the presented assay works by detecting the hydrogen peroxide by-product of an oxidase reaction (*Sm*NOX oxidizes NADH to NAD$^+$) using a cascade reaction catalyzed by HRP (**Figure 1B** right panel). Since in a typical droplet-based enzyme evolution experiment, both cell lysis and the enzymatic assay take place in the same environment, several additional components of the cascade reaction are required (**Table S1**) and none must interfere with the assay.[60] First, we determined the sensitivity of the assay in bulk experiments that were designed to imitate single droplets (for details, see **Section S4**). In short, the number of cells contained in a 100 µL reaction mix (lysis solution, assay components) is a scaled-up equivalent to a pL-volume droplet that contains a maximum of one cell. The background signal of lysed cells, present in droplet-based experiments, was imitated by adding *E. coli* cells that carried an empty pET28a vector and underwent the same expression protocol. Different activities of presumably expressed enzymatic variants were simulated by adding varying concentrations of purified *Sps*ADH, keeping the assay composition as close as possible to a droplet-based microfluidic experiment.

Since the assay is performed in the presence of lysed cells, NAD$^+$ is not only reduced by the enzyme of interest, but also by the native enzymes of the cell. This leads to a background signal that increases over time. Therefore, low activity enzyme variants need to be sufficiently distinguishable from the background signal to avoid sorting false negatives. **Figure 2A** shows that a stable linear increase of arbitrary fluorescence units (AFU) at low enzyme activities can be obtained. Therefore, a sufficiently long incubation time improves the signal with respect to the background fluorescence. At the same time, overoxidation of Amplex UltraRed to the non-fluorescent resazurin can occur due to a high initial or accumulated enzymatic activity over time. This phenomenon depicted in **Figure S4** demonstrates that at an enzymatic activity of 116 mU mL^{-1}, the fluorescence signal increases rapidly within 5 minutes. However, due to over-oxidation, it collapses and eventually saturates at AFU of about 3500. Meanwhile, at an enzymatic activity of 23.3 mU mL^{-1}, the fluorescent signal exhibits a saturation curve (without overoxidation), where saturation is reached at about 5000 AFU. Because of this overoxidation phenomenon, the proposed assay is best suited for enzymatic activities that are below 20 mU mL^{-1}. In FADS-based experiments using 5 pL droplets and based on estimations described in **Section S2**, this translates to about 31 mU mg^{-1}. **Figure 2B** shows the end point fluorescence signal at lower enzymatic activities after 2 hours of incubation time. The Z'-factor, an indicator of the applicability of an assay for high throughput screening[61], is 0.822 (more details in **Section S5**), indicating that the assay is suitable for activities as low as 0.06 mU mL^{-1}. According to the calculations presented in **Section S2**, this corresponds to about 0.1 mU mg^{-1} for a 5 pL droplet. As a final validation of the functionality of the assay we replicated the droplet screening process by lysing cells that expressed two enzyme variants with different specific activities in the assay mix instead of spiking with purified enzyme. Despite the low difference in activity (of approximately 3 mU mg^{-1}), there is no overlapping fluorescence signal after 10 minutes (for details, see **Section S6** and **Figure S5**). In addition, the preparation of the assay was performed in frozen single use aliquots, since it was observed that fluorescence sensitivity decreases with repeated freeze-thaw cycles (more information in **Section S7**).

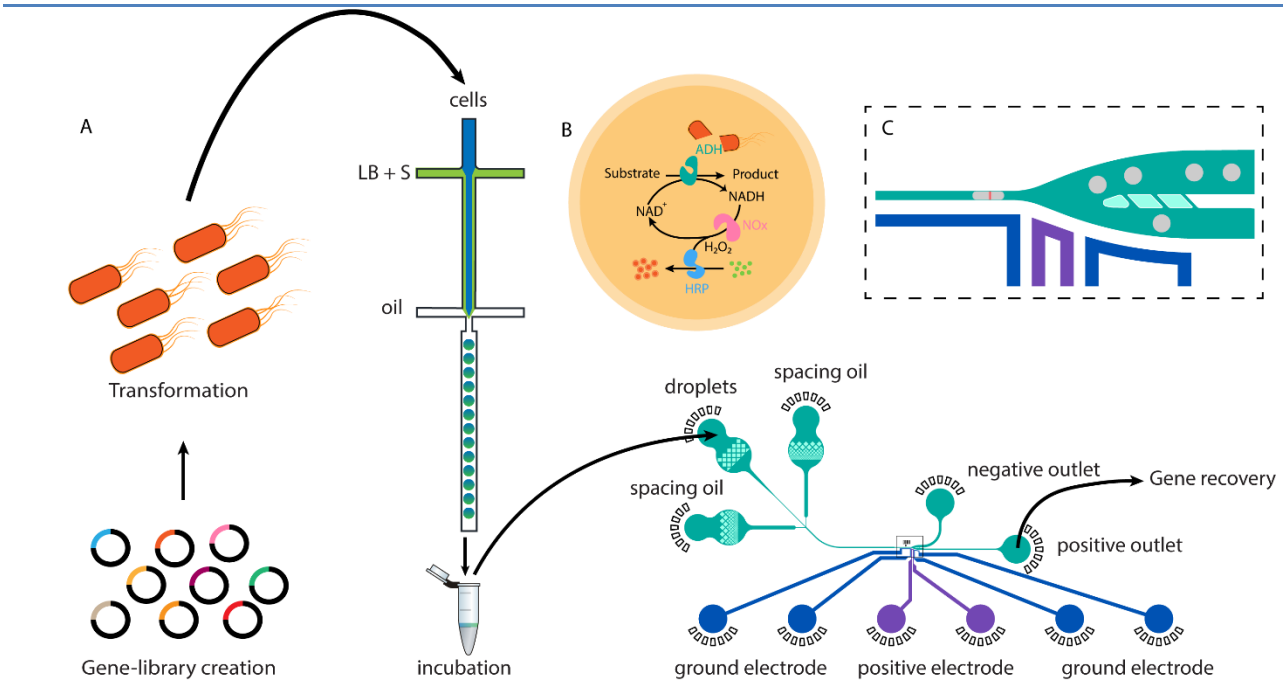

Figure 3. Overview of the experimental procedure using the droplet-based microfluidic platform. A) A library of mutant SpsADH was created and plasmids used to transform *E. coli* cells. Subsequently, droplets with individual cells, lysis buffer (LB) and substrate (S) were generated, incubated off-chip and then reinjected into the sorting chip. Droplets emitting fluorescence signals above a user-defined threshold were sorted and used for gene recovery. B) Schematic of the detection strategy for fluorescence-activated droplet sorting of ADH. C) Schematic representation of a typical microfluidic sorting chip.

Validation of the developed assay for the screening of mutant libraries in microdroplets

Considering the aforementioned optimization, we next used the assay to optimise the alcohol dehydrogenase *Sps*ADH, towards the non-native substrate L-guluronate (**Scheme 1**). To showcase that the assay is suitable even for very low activity enzymes, *Sps*ADH1, an engineered variant of *Sps*ADH with a specific activity of about 6 mU mg^{-1} at 10 mM l-guluronate (**Figure S2**) was taken as the template for the generation of the random mutagenesis library using error-prone PCR (epPCR) over the whole gene. This led to a gene library of about 5 x 10^4 variants present in E. coli NEB 10-beta and an average mutagenesis rate of 2.8 nucleotide exchanges per gene as determined by sequencing 10 variants. FADS experiments were then performed on this library, after transformation of E. coli BL21(DE3) cells and subsequent expression of the enzyme variants.

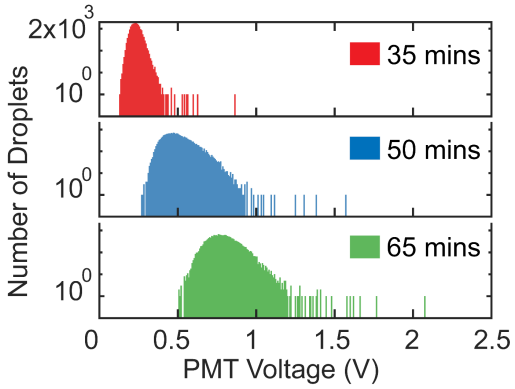

Figure 4. Characterization of the assay using the droplet-based microfluidic platform. The histograms show the fluorescent intensity of 20,000 screened droplets at different incubation times (36, 50 and 65 minutes). The appropriate incubation time of the assay can be chosen in any time-regime where the signal from the droplets shows an upward trend in fluorescence intensity.

The entire FADS screening process is depicted in **Figure 3**. Droplets with a volume of approximately 5 pL were formed at frequencies between 10 and15 kHz using a flow focusing geometry. A master mix containing the assay components and lysis agents was co-encapsulated with single cells expressing *Sps*ADH variants, adjusted to the cell concentration to yield a single cell occupancy of approximately 10%. After production, droplets were collected in an Eppendorf tube for varying incubation times at room temperature. The collected emulsion was then reinjected into a second microfluidic device (sorting chip), where droplets generating a fluorescence signal that exceeds a defined threshold were dielectrophoretically sorted and collected. As they moved downstream, fluorescence emission at 605 nm from each droplet was recorded using a photomultiplier tube (PMT) and excitation with a 532 nm laser (**Figure S6**). **Figure 4** shows the fluorescence intensity distribution of 20,000 individual droplets obtained at the corresponding time points. As the incubation time increases from 35 to 65 minutes, the average fluorescence intensity of the population increases gradually, defining the optimal incubation time range for the enzyme reaction prior to droplet sorting.

Since the average PMT voltage was constantly rising due to increase of the fluorescence product by catalysis of lysis components, the signal threshold for sorting was gradually adjusted during the entire sorting process, to avoid an

accumulation of false positives (**Figure S7**). Sorting was performed within a period of 30 minutes at a frequency of between 1 and 1.2 kHz. Considering that only 10 % of the droplets contained cells, 180,000 to 200,000 variants were screened within this period, leading to more than 3 times coverage of the whole library.

Hit validation and characterization

DNA from the positively sorted droplets were PCR amplified, cloned into an expression vector, inserted into the expression strain and subjected to a rescreen on a microtiter plate scale. Seven mutants could be confirmed as true positives with increased activity compared to *Sps*ADH1. All of them showed only a single nucleotide exchange, which interestingly were all in the 235th codon, (TTT to CTT and TTT to TTA), both leading to the amino acid exchange Phe235Leu. Compared to *Sps*ADH1, the enzymatic activity in the lysate based rescreen of the CTT mutant was increased 2.55-fold, while in the case of the TTA mutant the increase was 2.26-fold. Therefore, the improved variant CTT was selected for further kinetic characterization. The mutant was recombinantly expressed in *E. coli* BL21(DE3) and kinetic analysis (using a Michaelis Menten kinetic model) showed a minimal increase of k_{cat} by a factor of 1.1, while the K_m decreased by a factor of 2.3, leading to a 2.6-fold improvement in catalytic efficiency of the identified mutant compared to *Sps*ADH1 (**Figure S8**).

Based on the crystal structure of *Sps*ADH (PDB ID: 4TKM), the binding site is partially made up of an unresolved loop between amino acid 197 und 213 (**Figure S9**, dashed line).[62] Position 235 is located about 20 Å away on an alpha helix leading directly to this unresolved loop. Based on these observations, we can speculate that exchange of a phenylalanine residue with a leucine could potentially increase the stability of the helix[63], which in turn might stabilize the loop in a conformation that is beneficial for catalysis. Further studies are needed to validate this hypothesis.

CONCLUSION

In this work, we have described the development of an enzymatic fluorescence-based assay, for measuring activities of NAD$^+$-dependent enzymes, amenable to high-throughput enzyme engineering in FADS platforms. Compared to AADS platforms which rely on WST-1 absorbance detection, the presented assay benefits from the higher throughput and sensitivity of FADS systems. Bulk experiments showed that in the presence of a lysed cell background, the assay is capable of reliably detecting enzymes with activities as low as 0.06 mU mL^{-1}, while in 5 pL droplets used in FADS experiments, this corresponds to about 0.1 mU mg^{-1} (see **Section S2**).

We validated the utility of the assay by performing a DE experiment of an alcohol dehydrogenase from *Sphingomonas species* A1 towards the non-native catalysis of L-guluronate to D-glucarate. Although glucarate is considered to be one of the top value-added chemicals[52], its biocatalytic production has not yet been demonstrated by any enzyme despite the abundance of L-guluronate in macro algae as a suitable precursor. Our FADS platform was applied to a random mutagenesis library of 50,000 variants and identified two different variants with a synonymous mutation and having a 2.6-fold increase in catalytic efficiency with only a single round of mutagenesis and selection.

By detecting NADH formation, the use of this assay can be extended far beyond the screening and engineering of dehydrogenases to any reactions that can be coupled to a dehydrogenation step (**Figure 1**)[38,39]. Since the detection reaction converts NADH back to NAD$^+$, the oxidation step is irreversible and thus the assay even allows screening of enzymatic activities against the thermodynamic equilibrium of the reaction. The high sensitivity, however, comes with the drawback of fluorescence signal loss, as observed in the bulk experiments, when the initial activity of the target enzyme is too high due to further oxidation of the resorufin. Thus, when performing enzyme engineering, these bulk experiments can serve as a guide of how to adjust the assay to the properties of the target enzyme before conducting enzyme engineering in the FADS platform.

EXPERIMENTAL SECTION

Cells transformed with a library of *Sps*ADH variants, were expressed in *E. coli*. The master mix for the assay as well as all other components used are provided in **Table S1**. A droplet-based microfluidic device was used for single cell encapsulation in a lysis-assay mixed solution. Droplets were incubated in a reaction tube at room temperature for one hour before reinjection into a FADS device. Fluorescence was measured at an excitation wavelength of 532 nm. When the fluorescence signal surpassed a user-defined threshold, the corresponding droplet was sorted and collected in a reaction tube. PCR was performed on the positively sorted droplets by adding a NEB Q5 polymerase master mix into the reaction tube. The PCR products were ligated into expression vectors and subsequently cells were transformed using these vectors. Protein expression was performed in deep well plates. Using a liquid handling station, cells were lysed and the supernatant inspected for enzymatic activity using the WST-1 assay. Detailed information of all experimental procedures can be found in **Section S1**.

ASSOCIATED CONTENT

Supporting Information

The supporting information is available free of charge at …

AUTHOR INFORMATION

Corresponding Author

Volker Sieber – sieber@tum.de

Author Contributions

GK an VS perceived the study, GK developed and characterized the assay, DR provided the mutagenesis library, AJ and TB performed the microfluidic sorting experiment, LW and MD performed the robotic screening, DR and MS

characterized the enzymes and GK, AJ, TB, MS, BB, SS, AdM and VS wrote the manuscript. AJ and BB prepared the graphics. GK and AJ contributed equally.

Funding Sources

GK and MS were funded by the BMBF DIVE-IT grant No. 031B0615A. AJ was funded by the SNF grant No. 205321_176011

Notes

The authors declare no competing financial interest.

ACKNOWLEDGMENTS

We would like to thank Michel Richter and Josep Puig-martí-Luis for introducing the authors to each other.

ABBREVIATIONS

NAD(P), nicotinamide adenine dinucleotide (phosphate); *Sps*ADH, alcohol dehydrogenase from *Sphingomonas species* A1; FADS, fluorescence-activated droplet sorting; DE, directed evolution; HRP, horseradish peroxidase; EC, enzyme commission; AADS, absorbance-activated droplet sorting; NOX, NADH oxidase; WST-1 ((4-[3-(4-iodophenyl)-2-(4-nitrophenyl)-2H-5-tetrazolio]-1,3-benzol-disulfonate)), *Tt*NOX, NADH oxidase from *T. thermophilus* HB8; *Af*NOX, NADH oxidase from *A. fulgidus*, AFU, arbitrary fluorescent units; epPCR; error prone polymerase chain reaction; PMT, photon multiplier tube

REFERENCES

(1) Wohlgemuth, R. Biocatalysis-Key to Sustainable Industrial Chemistry. *Current Opinion in Biotechnology*. Elsevier Current Trends December 1, 2010, pp 713–724. https://doi.org/10.1016/j.copbio.2010.09.016.

(2) Sheldon, R. A.; Woodley, J. M. Role of Biocatalysis in Sustainable Chemistry. *Chemical Reviews*. American Chemical Society January 24, 2018, pp 801–838. https://doi.org/10.1021/acs.chemrev.7b00203.

(3) Sans, V. Emerging Trends in Flow Chemistry Enabled by 3D Printing: Robust Reactors, Biocatalysis and Electrochemistry. *Current Opinion in Green and Sustainable Chemistry*. Elsevier October 1, 2020, p 100367. https://doi.org/10.1016/j.cogsc.2020.100367.

(4) Porter, J. L.; Rusli, R. A.; Ollis, D. L. Directed Evolution of Enzymes for Industrial Biocatalysis. *ChemBioChem*. John Wiley & Sons, Ltd February 1, 2016, pp 197–203. https://doi.org/10.1002/cbic.201500280.

(5) Sheludko, Y. V.; Fessner, W. D. Winning the Numbers Game in Enzyme Evolution – Fast Screening Methods for Improved Biotechnology Proteins. *Curr. Opin. Struct. Biol.* **2020**, *63*, 123–133. https://doi.org/10.1016/j.sbi.2020.05.003.

(6) Victorino da Silva Amatto, I.; Gonsales da Rosa-Garzon, N.; Antônio de Oliveira Simões, F.; Santiago, F.; Pereira da Silva Leite, N.; Raspante Martins, J.; Cabral, H. Enzyme Engineering and Its Industrial Applications. *Biotechnology and Applied Biochemistry*. John Wiley & Sons, Ltd 2021. https://doi.org/10.1002/bab.2117.

(7) Bornscheuer, U. T.; Huisman, G. W.; Kazlauskas, R. J.; Lutz, S.; Moore, J. C.; Robins, K. Engineering the Third Wave of Biocatalysis. *Nature* **2012**, *485* (7397), 185–194. https://doi.org/10.1038/nature11117.

(8) Jackson, C. J.; Weir, K.; Herlt, A.; Khurana, J.; Sutherland, T. D.; Horne, I.; Easton, C.; Russell, R. J.; Scott, C.; Oakeshott, J. G. Structure-Based Rational Design of a Phosphotriesterase. *Appl. Environ. Microbiol.* **2009**, *75* (15), 5153–5156. https://doi.org/10.1128/AEM.00629-09.

(9) Öhlknecht, C.; Petrov, D.; Engele, P.; Krößl, C.; Sprenger, B.; Fischer, A.; Lingg, N.; Schneider, R.; Oostenbrink, C. Enhancing the Promiscuity of a Member of the Caspase Protease Family by Rational Design. *Proteins Struct. Funct. Bioinforma.* **2020**, *88* (10), 1303–1318. https://doi.org/10.1002/prot.25950.

(10) Yang, H.; Liu, L.; Li, J.; Chen, J.; Du, G. Rational Design to Improve Protein Thermostability: Recent Advances and Prospects. *ChemBioEng Rev.* **2015**, *2* (2), 87–94. https://doi.org/10.1002/cben.201400032.

(11) Dodda, S. R.; Sarkar, N.; Jain, P.; Aikat, K.; Mukhopadhyay, S. S. Improved Catalytic Activity and Stability of Cellobiohydrolase (Cel6A) from the Aspergillus Fumigatus by Rational Design. *Protein Eng. Des. Sel.* **2020**, *33*, 1–11. https://doi.org/10.1093/protein/gzaa020.

(12) Jumper, J.; Evans, R.; Pritzel, A.; Green, T.; Figurnov, M.; Ronneberger, O.; Tunyasuvunakool, K.; Bates, R.; Žídek, A.; Potapenko, A.; Bridgland, A.; Meyer, C.; Kohl, S. A. A.; Ballard, A. J.; Cowie, A.; Romera-Paredes, B.; Nikolov, S.; Jain, R.; Adler, J.; Back, T.; Petersen, S.; Reiman, D.; Clancy, E.; Zielinski, M.; Steinegger, M.; Pacholska, M.; Berghammer, T.; Bodenstein, S.; Silver, D.; Vinyals, O.; Senior, A. W.; Kavukcuoglu, K.; Kohli, P.; Hassabis, D. Highly Accurate Protein Structure Prediction with AlphaFold. *Nature* **2021**, *596* (7873), 583–589. https://doi.org/10.1038/s41586-021-03819-2.

(13) Wu, Z.; Jennifer Kan, S. B.; Lewis, R. D.; Wittmann, B. J.; Arnold, F. H. Machine Learning-Assisted Directed Protein Evolution with Combinatorial Libraries. *Proc. Natl. Acad. Sci. U. S. A.* **2019**, *116* (18), 8852–8858. https://doi.org/10.1073/pnas.1901979116.

(14) Mazurenko, S.; Prokop, Z.; Damborsky, J. Machine Learning in Enzyme Engineering. *ACS*

Catalysis. American Chemical Society January 17, 2020, pp 1210–1223. https://doi.org/10.1021/acscatal.9b04321.

(15) Kuchner, O.; Arnold, F. H. Directed Evolution of Enzyme Catalysts. *Trends in Biotechnology*. Elsevier Current Trends December 1, 1997, pp 523–530. https://doi.org/10.1016/S0167-7799(97)01138-4.

(16) Ye, L.; Yang, C.; Yu, H. From Molecular Engineering to Process Engineering: Development of High-Throughput Screening Methods in Enzyme Directed Evolution. *Applied Microbiology and Biotechnology*. Springer November 27, 2018, pp 559–567. https://doi.org/10.1007/s00253-017-8568-y.

(17) Manteca, A.; Gadea, A.; Van Assche, D.; Cossard, P.; Gillard-Bocquet, M.; Beneyton, T.; Innis, C. A.; Baret, J.-C. Directed Evolution in Drops: Molecular Aspects and Applications. *ACS Synth. Biol.* **2021**, acssynbio.1c00313. https://doi.org/10.1021/acssynbio.1c00313.

(18) Chiu, F. W. Y.; Stavrakis, S. High-throughput Droplet-based Microfluidics for Directed Evolution of Enzymes. *Electrophoresis* **2019**, elps.201900222. https://doi.org/10.1002/elps.201900222.

(19) Baret, J. C.; Miller, O. J.; Taly, V.; Ryckelynck, M.; El-Harrak, A.; Frenz, L.; Rick, C.; Samuels, M. L.; Hutchison, J. B.; Agresti, J. J.; Link, D. R.; Weitz, D. A.; Griffiths, A. D. Fluorescence-Activated Droplet Sorting (FADS): Efficient Microfluidic Cell Sorting Based on Enzymatic Activity. *Lab Chip* **2009**, *9* (13), 1850–1858. https://doi.org/10.1039/b902504a.

(20) Debon, A.; Pott, M.; Obexer, R.; Green, A. P.; Friedrich, L.; Griffiths, A. D.; Hilvert, D. Ultrahigh-Throughput Screening Enables Efficient Single-Round Oxidase Remodelling. *Nat. Catal.* **2019**, *2* (9), 740–747. https://doi.org/10.1038/s41929-019-0340-5.

(21) Kintses, B.; Hein, C.; Mohamed, M. F.; Fischlechner, M.; Courtois, F.; Lainé, C.; Hollfelder, F. Picoliter Cell Lysate Assays in Microfluidic Droplet Compartments for Directed Enzyme Evolution. *Chem. Biol.* **2012**, *19* (8), 1001–1009. https://doi.org/10.1016/j.chembiol.2012.06.009.

(22) Agresti, J. J.; Antipov, E.; Abate, A. R.; Ahn, K.; Rowat, A. C.; Baret, J. C.; Marquez, M.; Klibanov, A. M.; Griffiths, A. D.; Weitz, D. A. Ultrahigh-Throughput Screening in Drop-Based Microfluidics for Directed Evolution. *Proc. Natl. Acad. Sci. U. S. A.* **2010**, *107* (9), 4004–4009. https://doi.org/10.1073/pnas.0910781107.

(23) Ostafe, R.; Prodanovic, R.; Ung, W. L.; Weitz, D. A.; Fischer, R. A High-Throughput Cellulase Screening System Based on Droplet Microfluidics. *Biomicrofluidics* **2014**, *8* (4). https://doi.org/10.1063/1.4886771.

(24) Zinchenko, A.; Devenish, S. R. A.; Kintses, B.; Colin, P.-Y.; Fischlechner, M.; Hollfelder, F. One in a Million: Flow Cytometric Sorting of Single Cell-Lysate Assays in Monodisperse Picolitre Double Emulsion Droplets for Directed Evolution. *Anal. Chem.* **2014**, *86* (5), 2526–2533. https://doi.org/10.1021/ac403585p.

(25) Karamitros, C. S.; Morvan, M.; Vigne, A.; Lim, J.; Gruner, P.; Beneyton, T.; Vrignon, J.; Baret, J.-C. Bacterial Expression Systems for Enzymatic Activity in Droplet-Based Microfluidics. *Anal. Chem.* **2020**, *92* (7), 4908–4916. https://doi.org/10.1021/acs.analchem.9b04969.

(26) Prodanović, R.; Lloyd Ung, W.; Đurđić, K. I.; Fischer, R.; Weitz, D. A.; Ostafe, R. A High-Throughput Screening System Based on Droplet Microfluidics for Glucose Oxidase Gene Libraries. *Molecules* **2020**, *25* (10), 2418. https://doi.org/10.3390/molecules25102418.

(27) Najah, M.; Mayot, E.; Mahendra-Wijaya, I. P.; Griffiths, A. D.; Ladame, S.; Drevelle, A. New Glycosidase Substrates for Droplet-Based Microfluidic Screening. *Anal. Chem.* **2013**, *85* (20), 9807–9814. https://doi.org/10.1021/ac4022709.

(28) Fenneteau, J.; Chauvin, D.; Griffiths, A. D.; Nizak, C.; Cossy, J. Synthesis of New Hydrophilic Rhodamine Based Enzymatic Substrates Compatible with Droplet-Based Microfluidic Assays. *Chem. Commun.* **2017**, *53* (39), 5437–5440. https://doi.org/10.1039/c7cc01506b.

(29) Loo, B. van; Heberlein, M.; Mair, P.; Zinchenko, A.; Schüürmann, J.; Eenink, B. D. G.; Holstein, J. M.; Dilkaute, C.; Jose, J.; Hollfelder, F.; Bornberg-Bauer, E. High-Throughput, Lysis-Free Screening for Sulfatase Activity Using Escherichia Coli Autodisplay in Microdroplets. *ACS Synth. Biol.* **2019**, *8* (12), 2690–2700. https://doi.org/10.1021/ACSSYNBIO.9B00274.

(30) Klaus, M.; Zurek, P. J.; Kaminski, T. S.; Pushpanath, A.; Neufeld, K.; Hollfelder, F. Ultrahigh-Throughput Detection of Enzymatic Alcohol Dehydrogenase Activity in Microfluidic Droplets with a Direct Fluorogenic Assay. *ChemBioChem* **2021**. https://doi.org/10.1002/cbic.202100322.

(31) Colin, P. Y.; Kintses, B.; Gielen, F.; Miton, C. M.; Fischer, G.; Mohamed, M. F.; Hyvönen, M.; Morgavi, D. P.; Janssen, D. B.; Hollfelder, F. Ultrahigh-Throughput Discovery of Promiscuous Enzymes by Picodroplet Functional Metagenomics. *Nat. Commun.* **2015**, *6* (1), 10008. https://doi.org/10.1038/ncomms10008.

(32) Ma, F.; Chung, M. T.; Yao, Y.; Nidetz, R.; Lee, L. M.; Liu, A. P.; Feng, Y.; Kurabayashi, K.; Yang, G. Y. Efficient Molecular Evolution to Generate Enantioselective Enzymes Using a Dual-

Channel Microfluidic Droplet Screening Platform. *Nat. Commun.* **2018**, *9* (1), 1030. https://doi.org/10.1038/s41467-018-03492-6.

(33) Yang, J.; Tu, R.; Yuan, H.; Wang, Q.; Zhu, L. Recent Advances in Droplet Microfluidics for Enzyme and Cell Factory Engineering. *Critical Reviews in Biotechnology*. Taylor and Francis Ltd. 2021, pp 1023–1045. https://doi.org/10.1080/07388551.2021.1898326.

(34) Gielen, F.; Hours, R.; Emond, S.; Fischlechner, M.; Schell, U.; Hollfelder, F. Ultrahigh-Throughput–Directed Enzyme Evolution by Absorbance-Activated Droplet Sorting (AADS). *Proc. Natl. Acad. Sci.* **2016**, *113* (47), E7383–E7389. https://doi.org/10.1073/pnas.1606927113.

(35) Panke, S.; Held, M.; Wubbolts, M. Trends and Innovations in Industrial Biocatalysis for the Production of Fine Chemicals. *Current Opinion in Biotechnology*. Elsevier Current Trends August 1, 2004, pp 272–279. https://doi.org/10.1016/j.copbio.2004.06.011.

(36) Pick, A.; Rühmann, B.; Schmid, J.; Sieber, V. Novel CAD-like Enzymes from Escherichia Coli K-12 as Additional Tools in Chemical Production. *Appl. Microbiol. Biotechnol.* **2013**, *97* (13), 5815–5824. https://doi.org/10.1007/s00253-012-4474-5.

(37) Liese, A. (Andreas); Seelbach, K. (Karsten); Wandrey, C. *Industrial Biotransformations*; Wiley-VCH, 2006.

(38) GmbH., B. M. *Methods of Biochemical Analysis and Food Analysis Using Test-Combinations: Instructions for the Analysis of Foodstuffs, Chemicals, Cosmetics and Pharmaceuticals, Paper, Tobacco, Water, Animal Feed, Fertilizers, Biological Samples (Blood, Fermentation Solu*; Biochemical analysis : food analysis; Boehringer Mannheim, 1989.

(39) Russell Warnick, G.; Spain, M.; Kloepfer, H.; McMillan Volke, T. Standardization of a Commercial (Boehringer Mannheim Diagnostics) Enzymic Method for Cholesterol. *Clin. Chem.* **1989**, *35* (3), 409–413. https://doi.org/10.1093/clinchem/35.3.409.

(40) Hoffmann, G.; Bönsch, K.; Greiner-Stöffele, T.; Ballschmiter, M. Changing the Substrate Specificity of P450cam towards Diphenylmethane by Semi-Rational Enzyme Engineering. *Protein Eng. Des. Sel.* **2011**, *24* (5), 439–446. https://doi.org/10.1093/protein/gzq119.

(41) Abrahamson, M. J.; Vázquez-Figueroa, E.; Woodall, N. B.; Moore, J. C.; Bommarius, A. S. Development of an Amine Dehydrogenase for Synthesis of Chiral Amines. *Angew. Chemie - Int. Ed.* **2012**, *51* (16), 3969–3972. https://doi.org/10.1002/anie.201107813.

(42) Van Beek, H. L.; Romero, E.; Fraaije, M. W. Engineering Cyclohexanone Monooxygenase for the Production of Methyl Propanoate. *ACS Chem. Biol.* **2017**, *12* (1), 291–299. https://doi.org/10.1021/acschembio.6b00965.

(43) Zhang, D.; Chen, X.; Chi, J.; Feng, J.; Wu, Q.; Zhu, D. Semi-Rational Engineering a Carbonyl Reductase for the Enantioselective Reduction of β-Amino Ketones. *ACS Catal.* **2015**, *5* (4), 2452–2457. https://doi.org/10.1021/acscatal.5b00226.

(44) Fu, X.; Zhang, Y.; Xu, Q.; Sun, X.; Meng, F. Recent Advances on Sorting Methods of High-Throughput Droplet-Based Microfluidics in Enzyme Directed Evolution. *Frontiers in Chemistry*. Frontiers April 23, 2021, p 168. https://doi.org/10.3389/fchem.2021.666867.

(45) Chamchoy, K.; Pakotiprapha, D.; Pumirat, P.; Leartsakulpanich, U.; Boonyuen, U. Application of WST-8 Based Colorimetric NAD(P)H Detection for Quantitative Dehydrogenase Assays. *BMC Biochem.* **2019**, *20* (1), 1–14. https://doi.org/10.1186/s12858-019-0108-1.

(46) Zachos, I.; Genth, R.; Sutiono, S.; Marczynski, M.; Lieleg, O.; Sieber, V. Hot Flows: Evolving an Archaeal Glucose Dehydrogenase for Ultrastable Carba-NADP + Using Microfluidics at Elevated Temperatures. *ACS Catal.* **2022**, 1841–1846. https://doi.org/10.1021/acscatal.1c04320.

(47) Larsen, A. C.; Dunn, M. R.; Hatch, A.; Sau, S. P.; Youngbull, C.; Chaput, J. C. A General Strategy for Expanding Polymerase Function by Droplet Microfluidics. *Nat. Commun.* **2016**, *7* (1), 1–9. https://doi.org/10.1038/ncomms11235.

(48) Utech, S.; Prodanovic, R.; Mao, A. S.; Ostafe, R.; Mooney, D. J.; Weitz, D. A. Microfluidic Generation of Monodisperse, Structurally Homogeneous Alginate Microgels for Cell Encapsulation and 3D Cell Culture. *Adv. Healthc. Mater.* **2015**, *4* (11), 1628–1633. https://doi.org/10.1002/adhm.201500021.

(49) Althoff, E. A.; Wang, L.; Jiang, L.; Giger, L.; Lassila, J. K.; Wang, Z.; Smith, M.; Hari, S.; Kast, P.; Herschlag, D.; Hilvert, D.; Baker, D. Robust Design and Optimization of Retroaldol Enzymes. *Protein Sci.* **2012**, *21* (5), 717–726. https://doi.org/10.1002/pro.2059.

(50) Beer, B.; Pick, A.; Döring, M.; Lommes, P.; Sieber, V. Substrate Scope of a Dehydrogenase from Sphingomonas Species A1 and Its Potential Application in the Synthesis of Rare Sugars and Sugar Derivatives. *Microb. Biotechnol.* **2018**, *11* (4), 747–758. https://doi.org/10.1111/1751-7915.13272.

(51) Rowbotham, J. S.; Dyer, P. W.; Greenwell, H. C.; Theodorou, M. K. Thermochemical Processing of Macroalgae: A Late Bloomer in the Development of Third-Generation Biofuels?

Biofuels. Future Science LtdLondon, UK July 2012, pp 441–461. https://doi.org/10.4155/bfs.12.29.

(52) Werpy, T.; Petersen, G. Top Value Added Chemicals from Biomass: Volume I -- Results of Screening for Potential Candidates from Sugars and Synthesis Gas. Office of Scientific and Technical Information (OSTI). *Off. Sci. Tech. Inf.* **2004**, 69. https://doi.org/10.2172/15008859.

(53) Pick, A.; Schmid, J.; Sieber, V. Characterization of Uronate Dehydrogenases Catalysing the Initial Step in an Oxidative Pathway. *Microb. Biotechnol.* **2015**, *8* (4), 633–643. https://doi.org/10.1111/1751-7915.12265.

(54) Nowak, C.; Beer, B.; Pick, A.; Roth, T.; Lommes, P.; Sieber, V. A Water-Forming NADH Oxidase from Lactobacillus Pentosus Suitable for the Regeneration of Synthetic Biomimetic Cofactors. *Front. Microbiol.* **2015**, *6* (SEP), 957. https://doi.org/10.3389/fmicb.2015.00957.

(55) Rehn, G.; Pedersen, A. T.; Woodley, J. M. Application of NAD(P)H Oxidase for Cofactor Regeneration in Dehydrogenase Catalyzed Oxidations. *J. Mol. Catal. B Enzym.* **2016**, *134*, 331–339. https://doi.org/10.1016/j.molcatb.2016.09.016.

(56) Higuchi, M.; Shimada, M.; Matsumoto, J.; Yamamoto, Y.; Rhaman, A.; Kamio, Y. Molecular Cloning and Sequence Analysis of the Gene Encoding the H2O2-Forming NADH Oxidase from Streptococcus Mutans. *Biosci. Biotechnol. Biochem.* **1994**, *58* (9), 1603–1607. https://doi.org/10.1271/bbb.58.1603.

(57) Kengen, S. W. M.; Van Der Oost, J.; De Vos, W. M. Molecular Characterization of H2O2-Forming NADH Oxidases from Archaeogiobus Fulgidus. *Eur. J. Biochem.* **2003**, *270* (13), 2885–2894. https://doi.org/10.1046/j.1432-1033.2003.03668.x.

(58) Park, H. -J; Reiser, C. O. A.; Kondruweit, S.; Erdmann, H.; Schmid, R. D.; Sprinzl, M. Purification and Characterization of a NADH Oxidase from the Thermophile Thermus Thermophilus HB8. *Eur. J. Biochem.* **1992**, *205* (3), 881–885. https://doi.org/10.1111/j.1432-1033.1992.tb16853.x.

(59) Miller, N. J.; Rice-Evans, C.; Davies, M. J.; Gopinathan, V.; Milner, A. A Novel Method for Measuring Antioxidant Capacity and Its Application to Monitoring the Antioxidant Status in Premature Neonates. *Clin. Sci.* **1993**, *84* (4), 407–412. https://doi.org/10.1042/cs0840407.

(60) Janiesch, J. W.; Weiss, M.; Kannenberg, G.; Hannabuss, J.; Surrey, T.; Platzman, I.; Spatz, J. P. Key Factors for Stable Retention of Fluorophores and Labeled Biomolecules in Droplet-Based Microfluidics. *Anal. Chem.* **2015**, *87* (4), 2063–2067. https://doi.org/10.1021/ac504736e.

(61) Zhang, J. H.; Chung, T. D. Y.; Oldenburg, K. R. A Simple Statistical Parameter for Use in Evaluation and Validation of High Throughput Screening Assays. *J. Biomol. Screen.* **1999**, *4* (2), 67–73. https://doi.org/10.1177/108705719900400206.

(62) Takase, R.; Mikami, B.; Kawai, S.; Murata, K.; Hashimoto, W. Structure-Based Conversion of the Coenzyme Requirement of a Short-Chain Dehydrogenase/Reductase Involved in Bacterial Alginate Metabolism. *J. Biol. Chem.* **2014**, *289* (48), 33198–33214. https://doi.org/10.1074/jbc.M114.585661.

(63) Pace, C. N.; Scholtz, J. M. A Helix Propensity Scale Based on Experimental Studies of Peptides and Proteins. *Biophys. J.* **1998**, *75* (1), 422–427. https://doi.org/10.1016/s0006-3495(98)77529-0.

Table of Contents artwork